

Continuous and Discontinuous Phase Transitions in Quantitative Genetics: the role of stabilizing selective pressure

Annalisa Fierro^{1,2}, Sergio Coccozza³, Antonella Monticelli⁴, Giovanni Scala^{2,5}, and Gennaro Miele^{2,5}

¹ CNR-SPIN Complesso Univ. Monte S. Angelo, Via Cinthia, I-80126 Naples, Italy

² Dipartimento di Fisica, Università degli Studi di Napoli "Federico II",
Complesso Univ. Monte S. Angelo, Via Cinthia, I-80126 Naples, Italy

³ Dipartimento di Medicina Molecolare e Biotecnologie Mediche,
Università degli Studi di Napoli "Federico II", Naples, Italy

⁴ Istituto di Endocrinologia ed Oncologia Sperimentale, CNR Napoli, Naples, Italy and

⁵ INFN - Sez. Napoli, Complesso Univ. Monte S. Angelo, Via Cinthia, I-80126 Naples, Italy

(Dated: May 2, 2019)

By using the tools of statistical mechanics, we have analyzed the evolution of a population of N diploid hermaphrodites in random mating regime. The population evolves under the effect of drift, selective pressure in form of viability on an additive polygenic trait, and mutation. The analysis allows to determine a phase diagram in the plane of mutation rate and strength of selection. The involved pattern of phase transitions is characterized by a line of critical points for weak selective pressure (smaller than a threshold), whereas discontinuous phase transitions characterized by metastable hysteresis are observed for strong selective pressure. A finite size scaling analysis suggests the analogy between our system and the mean field Ising model for selective pressure approaching the threshold from weaker values. In this framework, the mutation rate, which allows the system to explore the accessible microscopic states, is the parameter controlling the transition from large heterozygosity (*disordered* phase) to small heterozygosity (*ordered* one).

The need of applying a statistical approach arises in physics when the global properties of ensembles containing a huge number of elementary constituents are studied. In this case, the behavior of the single element (microstate) is irrelevant in favor of more informative averages on the whole ensemble (macrostate). In this sense, the situation is strictly analogous in both Population and Quantitative Genetics, where the analysis of allele frequencies and phenotype distribution parameters is preferred to the genetic/phenotypic description of each individual. The analogy between Quantitative Genetics and thermodynamics, noted from the very beginning by R. A. Fisher himself [1], allowed to introduce a concept of entropy for Population Genetics which satisfies the analogous of H-theorem [2]. Such information entropy measure ensures an exact solution at statistical equilibrium [2–5]. This point of view can be alternatively seen by defining a free fitness, namely the entropy divided by population size plus the mean fitness. The free fitness is maximized at equilibrium when natural selection and drift (random sampling) are at work [2, 5], and provides an analogous of free energy in thermodynamics. For a summary of the correspondence between evolutionary dynamics and statistical physics see, for example, Table 1 of Ref. [4]. Following the above analogy, in Ref. [6] the authors study the evolution of a polygenic trait under stabilizing selection, mutation and genetic drift, following the evolution of the expectation of the trait mean, the genetic variance, and a measure of the expected heterozygosity. Interestingly, for population size N and mutation rate μ , such that $N\mu < 1/4$, the macroscopic quantities change their behavior showing a kind of *phase transition*. Moreover, abrupt and gradual changes in the optimum, as well as

changes in the strength of stabilizing selection seem to induce hysteresis phenomena, which can be understood imagining that the macroscopic trajectories keep memory of the underlying genetic states. In the present paper, we analyze such phase transition phenomena looking for a more detailed statistical mechanics description. To this aim, we follow the evolution of a stochastic model, extensively analyzed in the past years (see for instance Ref. [3], and references therein). It consists in a population of N diploid hermaphrodite individuals, reproducing in pairs in a random mating regime, evolving under the effect of drift, selective pressure in form of viability, and mutation. Following Wright's seminal paper [7], we consider M different biallelic genes additively combining on the character, and the individual viability following a Gaussian profile in the trait. The model differs from those of Ref. [4] for the large interval of mutation rate considered here, and for the chosen fitness of the phenotype. Furthermore, in our analysis, the size of the population N plays the same role of the finite dimension in a physical system.

Let us consider a system of N diploid individuals, sexually reproducing with random mating between any pairs of individuals. Each individual is represented by two sequences of M variables, σ_{kj} (where $k = 1, 2$ stands for the two genome replicas, and $j = 1, \dots, M$ runs on different loci). We refer to σ_{kj} as alleles, and assume that each allele can take two values, ± 1 . At each generation, all individuals are removed, and a new generation of same size N is formed by off-springs of the previous individuals. A mutation rate, μ , is introduced, as the probability of an allele to mutate at each generation ($\sigma_{kj} \rightarrow -\sigma_{kj}$). Similar models were studied in Ref.s [8, 9].

Let us denote the additive polygenic phenotype random variable with $p = \sum_{j=1}^M \sum_{k=1}^2 \sigma_{kj}$. A stabilizing selective pressure on such a phenotype can be implemented via the survival probability of an offspring, typically known as *viability*, $S(p) \equiv \mathcal{N}\omega \exp[-(p - p_m)^2 \omega^2 / 2]$, where \mathcal{N} is the suitable normalization constant, ω measures the *strength of selection*, and p_m stands for the optimum phenotype (hereafter, we choose for simplicity $p_m = 0$). For $\omega = 0$, there is no selective pressure, and all the microscopic states are equivalent. Whereas, for $\omega \rightarrow \infty$, the selective pressure is at maximum, and the only surviving individuals are those with $p = p_m$. Thus, in general, the effect of the selective pressure is to reduce the accessible phase space to those microscopic states satisfying *in probability* the constraint on the phenotype.

Let us denote with $\rho_{\text{in}}(j)$ the initial frequency of the allele “1” in locus j . We consider for simplicity a starting population where the M variants are ± 1 with equal probability, namely $\rho_{\text{in}}(j) = 0.5, \forall j = 1, \dots, M$. This ansatz does not restrict the generality of the analysis, in fact for finite populations, random drift rapidly homogenizes the initial distribution of allele frequencies, making the final results almost independent of the initial assumption on $\rho_{\text{in}}(j)$ [6].

To describe the macroscopic state of the system, we introduce the following quantity:

$$\bar{q} \equiv \frac{1}{M} \sum_{j=1}^M \langle |q(j)| \rangle, \quad (1)$$

with

$$q(j) \equiv \frac{1}{2N} \sum_{i=1}^N \sum_{k=1}^2 \sigma_{ik}(j), \quad (2)$$

where $\langle \dots \rangle$ stands for the average over ~ 30 initially identical realizations of the system (hereafter simply denoted by *ensemble* of populations). Note that the definition of \bar{q} is inspired by a statistical mechanics analogue. In fact, if the quantity $q(j)$ of Eq. (2) resembles the magnetization per spin of an Ising model of $2N$ spins, \bar{q} of Eq. (1) gives the average of the magnetization modulus once properly normalized [10]. Following the same analogy, we also introduce the *susceptibility*, as

$$\bar{\chi} \equiv \frac{1}{M} \sum_{j=1}^M \chi(j), \quad (3)$$

with $\chi(j) \equiv 2N (\langle q(j)^2 \rangle - \langle |q(j)| \rangle^2)$. It is interesting to note that the *magnetization* $q(j)$ of j -th locus is related to the *expected* heterozygosity (fraction of heterozygous individuals expected on the basis of Hardy-Weinberg equilibrium condition) in the same locus, denoted by $h_s(j)$, which is a more familiar quantity in the Population Ge-

netics context. Indeed, one can easily prove that

$$\begin{aligned} h_s(j) &\equiv \frac{1}{4N^2} \sum_{i,l=1}^N \sum_{k,n=1}^2 (1 - \delta_{\sigma_{ik}(j)\sigma_{ln}(j)}) = \\ &= \frac{1}{2} (1 - q(j)^2). \end{aligned} \quad (4)$$

It is worth observing, that in our case $h_s(j)$ essentially coincides with the *observed* heterozygosity (observed fraction of heterozygous individuals). From Eq. (4), we see that the minimum of magnetization corresponds to the maximum of heterozygosity, and vice-versa.

For any fixed set of parameters N , M , ω , and μ , we follow numerically the evolution of a given population till it asymptotically reaches a stationary state, which we refer to as *steady* state, where we evaluate \bar{q} and $\bar{\chi}$. Let us start by focusing our attention on the role played by mutation rate and selection strength only, and to this aim we fix the values of N and M . In general, the system reaches the steady state for values of generation number, which depend on ω and μ . Two different behaviors are observed in the regime of small and large selective pressure strength, respectively.

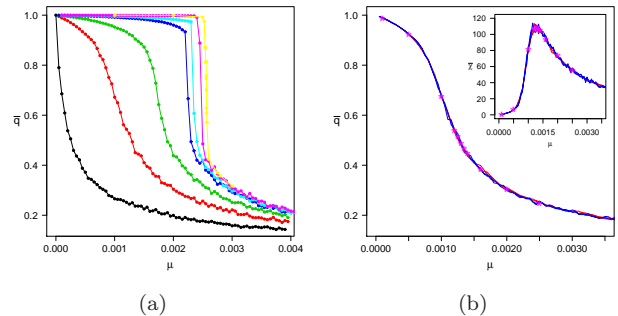


FIG. 1: (a) Order parameter, \bar{q} vs μ , in the steady states for $N = 1000$ and $\omega = 0, 0.1, 0.2, 0.4, 0.5, 1, \infty$ (from left to right). The continuous lines are guides for eyes. (b) Main frame: Order parameter, \bar{q} vs μ , for $\omega = 0.1$ and $N = 1000$. The full lines are obtained first cooling the system at fixed μ (the red line corresponds to 10^{-8} and the blue line to 10^{-9}), and then heating it at the same rate. The pink stars correspond to the steady states. Inset: Susceptibility, $\bar{\chi}$ vs μ , with the same symbols as in the main frame.

In Fig. 1(a), we report \bar{q} as a function of μ for different values of ω . As shown in figure, by decreasing the mutation rate μ , \bar{q} goes from small- \bar{q} (which vanishes in the limit of large- N) to $\bar{q} \sim 1$. Note that, for large μ , the alleles ± 1 have roughly equal probability (namely, $h_s(j) \sim 0.5$ for each locus), and hence the steady state does not significantly differ from the initial one. On the contrary, for small μ , in the steady state $h_s(j) \sim 0$ for each locus. In this case, the individuals

are just clones, namely, for each realization, the population is represented by a unique genome that is a generic combination of ± 1 in a neighborhood of the phenotype optimum (exactly in the optimum for $\omega \rightarrow \infty$). The crossover from the state with small \bar{q} (large heterozygosity) to the state with $\bar{q} \sim 1$ (small heterozygosity) is characterized by a maximum in the susceptibility, $\bar{\chi}$. The value of μ corresponding to such a maximum is a monotonic increasing function of ω . Moreover, concerning its dependence on M , it is interesting to observe that it simply scales as $1/M$, as one can expect since $2\mu M$, representing the mutation rate per individual, is the relevant quantity, ruling the mutations during evolution. From Fig. 1(a), it can be easily observed that for weak selection strength, namely $\omega \leq 0.4$ (blue circles in figure corresponding to $\omega = 0.4$), one has a smooth crossover that becomes abrupt for larger ω .

To better analyze the nature of these steady states, and the crossover from small- \bar{q} states to large- \bar{q} ones, we perform the following numerical experiment. For any value of ω , starting from a configuration at high mutation rate, we decrease μ at a given rate $\dot{\mu} \equiv \Delta\mu/\Delta n$ (n denoting the generation number). In other words, the system is kept at a given value of the mutation rate for an interval Δn , and, at the end of it, \bar{q} and $\bar{\chi}$ are measured. Afterward, the value of μ is decreased of $\Delta\mu$ and the procedure is iterated till μ reaches zero. At this point the procedure is inverted and μ is increased at the same rate, in analogy to a physical system, first cooled and then heated at given rate. For any μ , two states are considered macroscopically equivalent if the measured values of \bar{q} and $\bar{\chi}$ coincide, in analogy with a thermodynamical approach. This procedure confirms the presence of two different regimes, for $\omega < \omega_c$ and $\omega \geq \omega_c$, respectively, where the threshold $\omega_c \simeq 0.4 + \mathcal{O}(N^{-1})$.

In the region of small selective pressure, namely for $\omega < \omega_c$, plotting \bar{q} as function of μ , for small enough values of the cooling rate, $\dot{\mu}$, we find that the curve does not depend on $\dot{\mu}$ at all, and the two branches, obtained by decreasing and increasing μ respectively, always coincide. In the main frame of Fig. 1(b), \bar{q} vs μ is plotted for two different values of the cooling rate, and assuming $\omega = 0.1$. Similar behaviors are observed plotting $\bar{\chi}$ vs μ (see the inset of Fig. 1(b)). Moreover, the states obtained with this procedure coincide with the above defined steady states (pink stars in Fig. 1(b)), and in some sense they can be considered *equilibrium* states of the system. In this region, the crossover from large to small heterozygosity, ruled by the mutation rate and characterized by a susceptibility maximum, strongly resembles a continuous (second order) transition in a physical system. In the following, we will study this transition as a usual critical phenomenon [11].

From the intersection of the fourth order cumulant [11], evaluated for different sizes of the system, the critical mutation rate, $\mu_c \equiv \lim_{N \rightarrow \infty} \mu_c(N)$, is estimated (see Sup-

plementary Material [12] for further details), and a finite size scaling analysis is performed in order to evaluate the critical exponents of the transition. In Supplementary Material [12], $N^a \bar{q}$ and $N^{-b} \bar{\chi}$ are plotted, for a given ω , vs $N^c(\mu - \mu_c)/\mu_c$, where the exponents a , b , and c are chosen in order to rescale the curves for different N onto a unique curve. In a d -dimensional system, a , b and c are related to the critical exponents, ν , β and γ , by the following relations [11]: $a = \beta/\nu d$, $b = \gamma/\nu d$, and $c = 1/\nu d$. Although the space dimension is here not defined at all, we can evaluate β and γ , from a , b and c , as $\beta = a/c$ and $\gamma = b/c$. In Table I, μ_c and the scaling exponents obtained for different ω are listed. Although the errors are rather large and further analysis is necessary, the critical exponents seem to change along the critical line, and to tend to the mean field Ising critical exponents (i.e., $\beta = 0.5$ and $\gamma = 1$) by approaching ω_c . We can speculate that the role of the euclidean dimension is here played by the selective pressure, which controls the *energy* landscape of the system (the increasing of ω corresponds to an increasing of the energy barriers between two minima).

A different discussion deserves the system in absence of selective pressure (i.e., $\omega = 0$). In this case, in the limit of large- N , no transition is observed for finite mutation rate: the fourth order cumulant for different sizes has no intersection at finite μ , and $\mu_c(N)$ (the maximum point of the susceptibility at finite N) vanish as $1/N$ in the limit of large- N (data shown in Supplementary Material [12]). Similar findings are obtained for $\omega = 0.01$. Finally, in absence of selective pressure, since the loci are independent, there is no dependence on M at all.

ω	$\mu_c(\pm 0.00005)$	a	b	c	β	γ
0	0	0	1	1	0	1
0.05	0.00065	0.15	0.7	0.5	0.3	1.4
0.1	0.0014	0.175	0.65	0.5	0.35	1.3
0.13	0.0017	0.2	0.6	0.5	0.4	1.2
0.2	0.0021	0.25	0.6	0.5	0.5	1.2

TABLE I: Critical mutation rate and scaling exponents, for different ω , are reported. Note that the scaling relation $2\beta + \gamma = \nu d$, which in terms of a and b becomes $2a + b = 1$, is almost everywhere verified. Note that the uncertainty on the a , b and c determination is ~ 0.05 , whereas the error on β and γ estimations are ~ 0.1 and ~ 0.2 , respectively.

Interestingly, in the region of large selective pressure, for $\omega \geq \omega_c$, a metastable hysteresis appears between small values of \bar{q} and 1, as shown in Fig. 2(a). Again, for large mutation rate, the system is at equilibrium in states with small- \bar{q} , and, for small mutation rate, is at equilibrium in states with $\bar{q} \sim 1$. However, the two branches, at small- \bar{q} and $\bar{q} \sim 1$ respectively, are both observed for intermediate values of the mutation rate, depending on the pattern of μ -variation. Although by decreasing the cooling rate the hysteresis cycle shrinks, we always

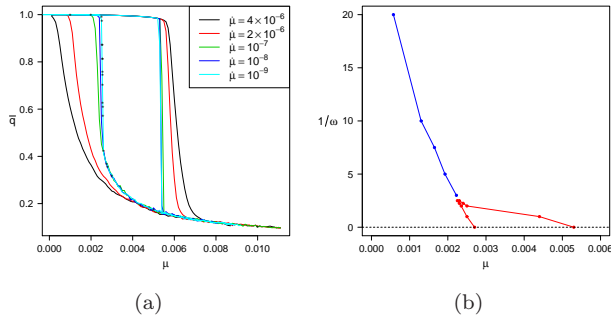


FIG. 2: (a) Order parameter, \bar{q} vs μ , for $N = 1000$ and $\omega \rightarrow \infty$. The different cycles have been obtained by using different cooling rates. The black stars reproduce data plotted in Fig. 1(a) for $\omega \rightarrow \infty$, obtained by following the system up to $2 \cdot 10^6$ generation numbers. (b) Phase diagram in the plane $(\mu, 1/\omega)$ for a system of size $N = 1000$ (see text for explanations). The continuous lines are guides for eyes.

see two well distinct branches on our observation time scales. This behavior is reminiscent of a discontinuous (first order) transition, where metastable hysteresis is usually observed. In this case, the distinction of long-lived metastable states from equilibrium states is rather difficult, since the lifetime of the metastable states may be longer than the observation time. As it can be seen in Fig. 2(a), the states, obtained decreasing μ at small $\dot{\mu}$, coincide with the steady states, reached by the system for very large generation numbers. Hence, in this case the so-called steady states, which are stationary on our observation time scales, are likely metastable. Note that in Fig. 2(a) the hysteresis curves are plotted for $\omega \rightarrow \infty$, where this phenomenon is more evident.

Our findings are efficaciously summarized in Fig. 2(b), where the phase diagram for a system of $N = 1000$ individuals is shown in the plane $(\mu, 1/\omega)$. For $\omega < \omega_c$, we plot $1/\omega$ as function of the maximum point of $\bar{\chi}$, $\mu_c(\omega, N)$ (for the dependence of $\mu_c(\omega, N)$ on N see Supplementary Material [12]). The blue line should give, in the *thermodynamic* limit, a line of critical points, where the continuous transition from small- \bar{q} to $\bar{q} = 1$ phase should be observed. Above ω_c , data depend on the cooling rate and the susceptibility displays two maxima, depending on the pattern of μ -variation. Red circles in Fig. 2(b) correspond to the maximum points of $\bar{\chi}$, along the hysteresis loop obtained at cooling rate $\dot{\mu} = 10^{-9}$. In this region, the system behaves as a physical system undergoing a discontinuous transition controlled by the mutation rate.

In Supplementary Material [12], the above analysis about the behavior of \bar{q} is carried out for the expected heterozygosity of the single population, \bar{H}_s , and for the expected heterozygosity measured on the set of popu-

lations as a whole, \bar{H}_t , as well. It is found that, for small mutation rate, the equilibrium state corresponds to $\bar{H}_s \sim 0$ and $\bar{H}_t \sim 0.5$, showing that from the initial identity (symmetry) among populations, due simply to stochasticity, eventually emerges a genetic diversity. This can be understood by thinking that below the critical mutation rate, each independent population reaches fixation ($\bar{H}_s \sim 0$) in generally different microstates ($\bar{H}_t \neq 0$). In our opinion, this phenomenon seems analogous to *spontaneously symmetry breaking* in physical system. As for the order parameter \bar{q} , metastable hysteresis is observed in both \bar{H}_s and \bar{H}_t for $\omega \geq \omega_c$.

In summary, in this paper we have analyzed the evolution of a population of N diploid individuals, sexually reproducing with random mating, evolving under the effect of a Gaussian viability depending on a polygenic additive trait. Using the standard tools of Statistical Mechanics, we show that the system displays a complex phase diagram with a transition from a disordered to an ordered phase, controlled by the mutation rate. We provide the phase diagram in the (μ, ω) plane, showing that the order of the transition changes depending on the strength of selection, being continuous for weak selective pressures and discontinuous for strong ones.

Acknowledgments The authors would like to thank L. Peliti and A. Coniglio for valuable discussions.

-
- [1] R.A. Fisher, in *The Genetical Theory of Natural Selection*, (Clarendon, Oxford, 1930).
 - [2] Y. Iwasa, *J. Theor. Biol.* **135**, 265 (1988).
 - [3] N.H. Barton, *Genetical Research* **54** 59 (1989).
 - [4] G. Sella and A.E. Hirsh, *Proc. Natl. Acad. Sci. U.S.A.*, **102**, 9541 (2005).
 - [5] N.H. Barton, J.B. Coe, *Jour. of Theor. Biology*, **259**, 317 (2009).
 - [6] H.P. de Vladar, N.H. Barton, *J R Soc Interface*, **8**, 720 (2011).
 - [7] S. Wright, *Genetics* **16**, 16 (1931).
 - [8] M. Serva and L. Peliti, *J. Phys. A: Math. Gen.* **24** (1991) L705.
 - [9] P.G. Higgs and B. Derrida, *J. Phys. A: Math. Gen.* **24** (1991) L985.
 - [10] For vanishing magnetic field ($H = 0$) the Ising model undergoes a second order phase transition from a disordered paramagnetic phase (vanishing magnetization) to an ordered ferromagnetic one (not vanishing magnetization), at temperature T_c . In the ferromagnetic phase ($T \leq T_c$), the magnetization $\rightarrow 0$ at the critical temperature as a power law with exponent β . For fixed temperature $T < T_c$, a first order transition controlled by the magnetic field, is found for vanishing H .
 - [11] K. Binder *Z. Phys. B Condensed Matter* 1981, **43** 119; D.L. Landau and K. Binder, in *A Guide to Monte-Carlo Simulations in Statistical Physics*, (CUP 2013).
 - [12] See Supplemental Material at <http://> for further details.

Continuous and Discontinuous Phase Transitions in Quantitative Genetics: the role of stabilizing selective pressure. Supplementary Material

Annalisa Fierro^{1,2}, Sergio Coccozza³, Antonella Monticelli⁴, Giovanni Scala^{2,5}, and Gennaro Miele^{2,5}

¹ CNR-SPIN Complesso Univ. Monte S. Angelo, Via Cinthia, I-80126 Naples, Italy

² Dipartimento di Fisica, Università degli Studi di Napoli "Federico II",
Complesso Univ. Monte S. Angelo, Via Cinthia, I-80126 Naples, Italy

³ Dipartimento di Medicina Molecolare e Biotecnologie Mediche,
Università degli Studi di Napoli "Federico II", Naples, Italy

⁴ Istituto di Endocrinologia ed Oncologia Sperimentale, CNR Napoli, Naples, Italy and

⁵ INFN - Sez. Napoli, Complesso Univ. Monte S. Angelo, Via Cinthia, I-80126 Naples, Italy

(Dated: May 2, 2019)

FINITE SIZE SCALING

In order to estimate the critical mutation rate μ_c , we calculate the fourth order cumulant for different size N of the system.

For an Ising model with vanishing magnetic field, the reduced fourth order cumulant of the order parameter [1] is given by

$$U_4 = 1 - \frac{\langle m^4 \rangle}{3\langle m^2 \rangle^2}, \quad (1)$$

where m is the magnetization. A natural extension of the above quantity to our system is

$$\bar{U}_4 \equiv \frac{1}{M} \sum_{j=1}^M U_4(j), \quad (2)$$

where

$$U_4(j) = 1 - \frac{\langle q(j)^4 \rangle}{3\langle q(j)^2 \rangle^2} \quad (3)$$

is the fourth order cumulant of j -th locus, $\langle \dots \rangle$ stands for the *ensemble* average as defined in the main text, and \bar{U}_4 denotes the average over the M loci.

Following Ref. [1], for an Ising model with vanishing magnetic field, as the system size $N \rightarrow \infty$, $U_4 \rightarrow 0$ for $T > T_c$ and $U_4 \rightarrow 2/3$ for $T < T_c$. For large enough values of the size N , all curves representing U_4 as a function of temperature cross in a point whose location gives the critical point. In the present case, increasing the mutation rate, in each locus j it is observed a transition from a disordered phase to an ordered one. This is in perfect analogy with the Ising model. Hence, we expect that varying the size N of the system, all curves for \bar{U}_4 as a function of μ cross in a point which provides the critical mutation rate $\mu_c \equiv \lim_{N \rightarrow \infty} \mu_c(N)$. Note that μ_c keeps a dependence on ω .

In Fig. 1, \bar{U}_4 is plotted as a function of μ for different values of the size N , having fixed $\omega = 0.2$. As expected, in the limit of large N , we find that \bar{U}_4 tends to $2/3$ and to zero for small and large mutation rate, respectively. The crossing point, μ_c , represented by the red circles in

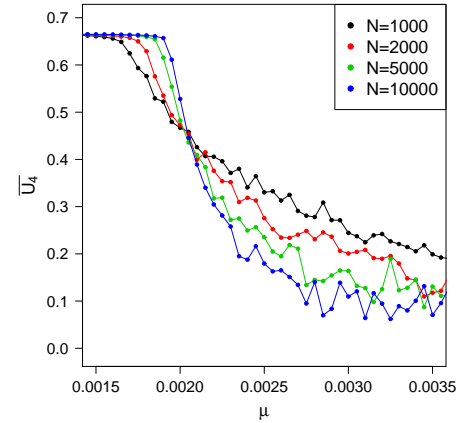


FIG. 1: \bar{U}_4 plotted as function of μ , for $\omega = 0.2$ and different values of N . The crossing point is $\mu_c \sim 0.0021$. The continuous lines are guides for eyes.

Fig. 2, increases by increasing ω and vanishes in the limit $\omega \rightarrow 0$. Blue stars in the same figure correspond to the maximum points of the susceptibility, namely $\mu_c(N)$ for $N = 1000$. We find that $\mu_c(N)$ is smaller than μ_c for each non vanishing ω , whereas this behavior reverses for $\omega = 0$, confirming that the case with no selective pressure is a peculiar one.

Next, the critical behaviors of the order parameter and of the susceptibility are studied. Extending the predictions from finite size scaling analysis in the Ising model [1] to the present system, we expect that near the critical point

$$\begin{aligned} \bar{q} &= N^{-a} q_0(\epsilon N^c), \\ \bar{\chi} &= N^b \chi_0(\epsilon N^c), \end{aligned} \quad (4)$$

where $\epsilon = (\mu - \mu_c)/\mu_c$, and q_0 and χ_0 are scaling functions. In a d -dimensional system, a , b and c are related to the usual critical exponents, ν , β and γ , by the following relations: $a = \beta/\nu d$, $b = \gamma/\nu d$, and $c = 1/\nu d$. In Figs 3 and 4, $N^a \bar{q}$ and $N^{-b} \bar{\chi}$ are plotted for $\omega = 0.2$ and 0.05 respectively, as a function of ϵN^c , where the exponents

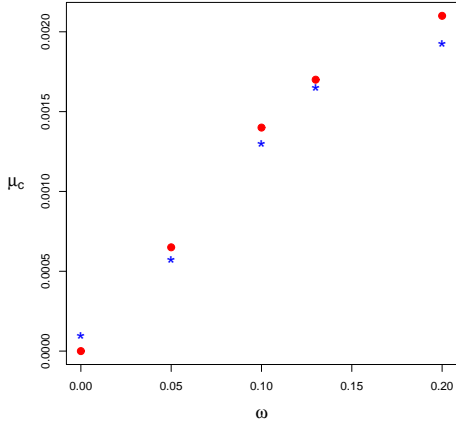


FIG. 2: Critical mutation rate, μ_c , (red circles) as a function of ω , compared with $\mu_c(N)$, for $N = 1000$ (blue stars).

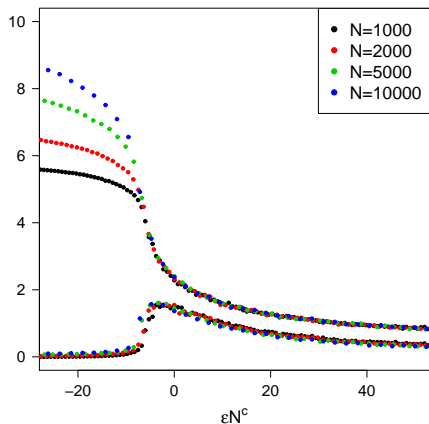


FIG. 3: $N^a \bar{q}$ (upper curves) and $N^{-b} \bar{\chi}$ (lower curves) plotted for $\omega = 0.2$ and different values of N , as a function of ϵN^c . In this case, we have $a = 0.25$, $b = 0.6$, $c = 0.5$, $\epsilon = (\mu - \mu_c)/\mu_c$ and $\mu_c = 0.0021$.

a , b , and c are chosen in order to rescale the curves for different N onto a unique one. As it is clear from Figs 3 and 4, a departure from scaling laws, Eq. (4), observed for $\mu < \mu_c$, is more evident for larger values of ω . The reason is that, increasing ω , for small mutation rate the system quickly becomes fully ordered (i.e., $\bar{q} \sim 1$), and the scaling does not hold.

As we have emphasized above, for $\omega = 0$, no crossing point is observed in the fourth order cumulant. Consistently, the maximum point of the susceptibility $\mu_c(N)$ goes to zero as $1/N$ (see inset of Fig. 5) in the limit $N \rightarrow \infty$, and, as it is shown in main frame of Fig. 5, the

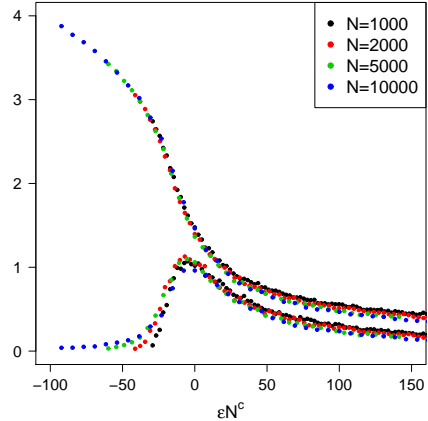


FIG. 4: $N^a \bar{q}$ (upper curves) and $N^{-b} \bar{\chi}$ (lower curves) plotted for $\omega = 0.05$ and different values of N , as a function of ϵN^c . In this case, we have $a = 0.15$, $b = 0.7$, $c = 0.5$, $\epsilon = (\mu - \mu_c)/\mu_c$ and $\mu_c = 0.00065$.

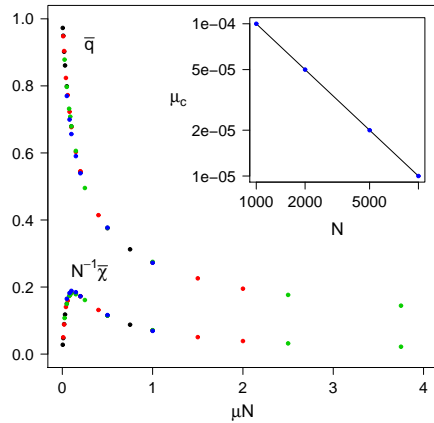


FIG. 5: **Main frame:** \bar{q} and $N^{-1} \bar{\chi}$, plotted as function of μN , for $\omega = 0$, and $N = 1000, 2000, 5000, 10000$. **Inset:** Critical mutation rate, $\mu_c(N)$, as function of N . The full line is the power law A/N , with $A \sim 0.1$.

following trivial finite size scaling is found:

$$\begin{aligned} \bar{q} &= q_0(\mu N), \\ \bar{\chi} &= N \chi_0(\mu N). \end{aligned} \quad (5)$$

HETEROZYGOSITY

Let us remind the for each set of parameters, we follow the evolution of $N_p = 30$ initially identical populations, which evolve independently. In order to evaluate the heterozygosity, we measure two quantities, which give

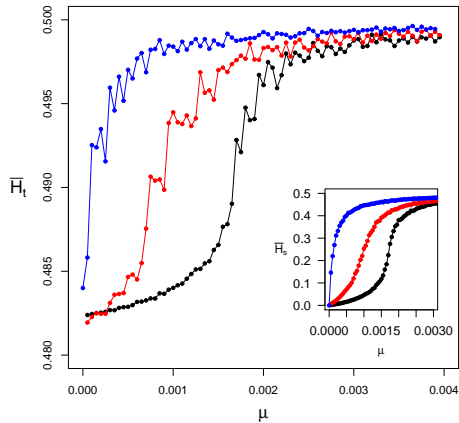


FIG. 6: **Main frame:** \overline{H}_t for $N = 1000$ and $\omega = 0, 0.1, 0.2$ (from left to right). **Inset:** \overline{H}_s for $N = 1000$ and $\omega = 0, 0.1, 0.2$ (from left to right). The continuous lines are guides for eyes.

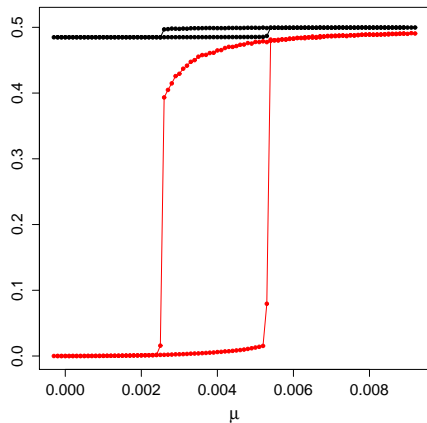


FIG. 7: The heterozygosities \overline{H}_s (red circles) and \overline{H}_t (black circles), for $N = 1000$ and $\omega \rightarrow \infty$, obtained first decreasing and then increasing, μ , at rate $\dot{\mu} = 10^{-9}$. The continuous lines are guides for eyes.

in some sense complementary information on the state of the system: the expected heterozygosity measured on the set of populations as a whole, \overline{H}_t , and the expected heterozygosity of the single population, \overline{H}_s , evaluated as the average of $h_s(j)$, Eq. (4) of the main text, over different loci and on the ensemble. One can easily prove that

$$\overline{H}_s = \frac{1}{2} \left(1 - \frac{\overline{\chi}}{2N} - \overline{q}^2 \right) \quad (6)$$

for a very large number of realizations. This occurs since, in this limit, $\langle |q(j)| \rangle$ is independent of j . From this equation, due to the scaling behaviors of \overline{q} and $\overline{\chi}$ for $\omega = 0$, we easily see that \overline{H}_s results scale free in absence of selective pressure.

As we can see from Figs 6 and 7, we find that the equilibrium state for large mutation rate corresponds to $\overline{H}_s \sim 0.5$ and $\overline{H}_t \sim 0.5$, and for small mutation rate to $\overline{H}_s \sim 0$ and $\overline{H}_t \sim 0.5$ (we expect $\overline{H}_t = 0.5$ for $N_p \rightarrow \infty$). This means that initially identical populations develop a genetic diversity below the critical mutation rate, since they reach fixation in, generally different but macroscopically equivalent, microstates. This phenomenon is analogous of the spontaneously symmetry breaking in physical system.

As for the order parameter \overline{q} , metastable hysteresis for \overline{H}_s and \overline{H}_t is observed for $\omega \geq \omega_c$ as well (see Fig. 7).

-
- [1] K. Binder *Z. Phys. B Condensed Matter* 1981, **43** 119; D.L. Landau and K. Binder, in *A Guide to Monte-Carlo Simulations in Statistical Physics*, (Cambridge University Press 2013).